A Comparative Study of Omega RSM and RNG k–ε Model for the Numerical Simulation of a Hydrocyclone

Zhuo Lun Cen*+; Ji Gang Zhao; Ben Xian Shen

State Key Laboratory of Chemical Engineering, East China University of Science and Technology,
Shanghai, 200237, CHINA

ABSTRACT: *The design and optimization of hydrocyclones using CFD techniques are gaining popularity and the key to a successful simulation lies with the accurate description of the high turbulent swirling behavior of the flow. This paper presents a detailed comparison between the Omega RSM and the RNG k–ε turbulence model, which are both derived specially for modeling swirling or rotational flow, in the simulation of a hydrocyclone. The predictions of velocity field, volume of vortexes, mass split and turbulent viscosity were obtained and compared. It is showed that in general both models gave similar predictions of the flow field under different inlet velocities, while the predictions of turbulent viscosity and in the core region of hydrocyclone were found more closely aligned with the reality using Omega RSM.*

KEY WORDS: *CFD, Hydrocyclone, RSM, RNG k–ε model, Fluent.*

INTRODUCTION

Hydrocyclones, wide-applied mechanical separation equipments, employ a centrifugal force to separate two phases with different densities. It has been developed rapidly in recent decades, for its exclusive advantages of no moving parts, simple structure, easy operation and less expensive device. Originally hydrocyclones were widely spread in solid-liquid separation since invented by *Bretney* in 1891. Until 1980s the application of hydocyclones in liquid-liquid separation became common, major in the separation of oil/water for the exploitation of crude oil [1-3]. Benefited from its high-efficiency and low-cost, liquid-liquid hydrocyclones have fast become a hot topic in the petrochemical industry. In Fig. 1, a profile of typical liquid-liquid hydocyclone, a cylinder on a cone part with an underflow tube,

is sketched with main streams. In all, the inlet flow is separated to two reversed streams, the overflow and the underflow. Though the functional principle and structure of hydrocyclones are quite simple, the flow field inside, the inner and outer vortexes, are fairly complicated due to the strong swirling movement and high turbulence.

CFD has a great potential to predict the flow field features inside the hydrocyclones [4]. The complicated flow in hydrocyclones places great demands on the numerical techniques and the turbulence models [5]. In this study, the CFD calculations were carried out using commercial finite volume code Ansys Fluent 14.0, which is ideally suited for incompressible to mildly compressible flows. For the high swirling turbulent flow in hydrocyclones, the key to a successful CFD simulation extremely lies with
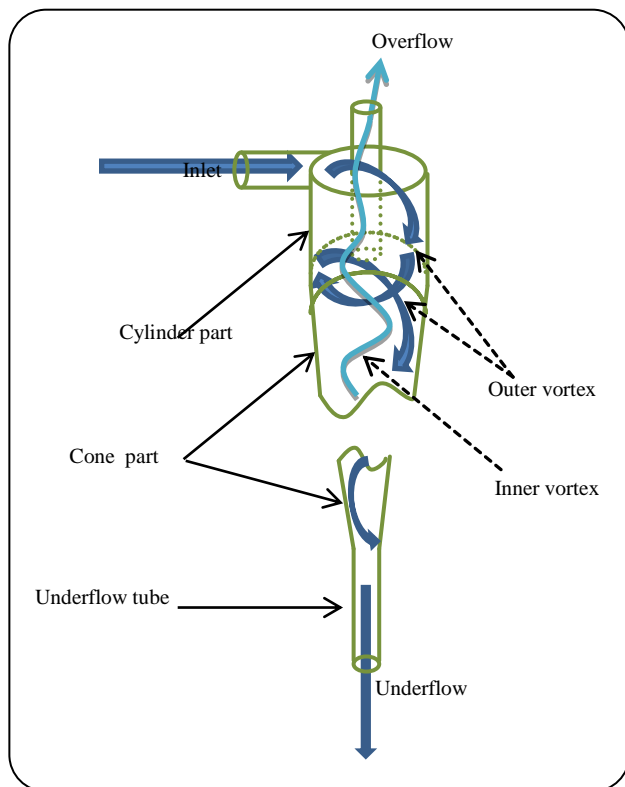
Fig. 1: A typical hydrocyclone for liquid-liquid separation, a cylinder part on a cone part with an underflow tube, with main streams: inlet, underflow, overflow.

the accurate selection of the turbulence model. A number of turbulence models are provided in Fluent and these range from the k-ε model to the more complicated Reynoleds Stress Model (RSM). Besides, both of them have a variety of derivative models applicable to different cases. The k-ε model has become the most popular in industrial flow simulation because of its robustness, economy, and reasonable accuracy for a wide range of turbulent flows, since it was proposed by Launder and Spalding [6]. RNG k-ε model is derived from standard k-ε with a modified turbulent viscosity that takes effect for axisymmetric, swirling flows and three-dimensional flows. Likewise, a derivation of RSM, with a Stress-Omega term based on the equations and LRR model, is provided for modeling flows over curved surfaces and swirling flows specially [7].

Few investigations have been carried out, for the application of Omega RSM to the numerical simulation on hydrocyclones that feature a swirling-dominated and high turbulent flow. In this study, both the Stress-Omega Reynolds Stress Model (Omega RSM) and the RNG k-ε

model were introduced to simulate the flow field inside the liquid-liquid hydrocyclone. The predictions of flow field and mass split ratio obtained by two models were compared and analyzed in details. These may enhance our understanding of the distinctions between two models and can also provide references for the CFD study of other industrial processes characterized by high turbulent swirling flow.

THEORITICAL SECTION
CFD modeling

CFD is a mathematical way to represent the real flow field in the form of a set of conventional conservation equations. The incompressible Navier -Stokes equations are appropriate for the numerical simulation on the flow inside the hydrocyclone. In addition to this, an extra turbulence model that can represent the Reynolds stress term, $\rho\overline{\mu_t\mu_j}$, is required to enclose the Navier-Stokes equations. In Fluent several different turbulence models are available to available. The ones in use for engineering applications are k-ε model and Reynolds stress model. In this paper, CFD predictions with two turbulence models, RNG k-ε model and Stress-Omega Reynolds stress model that are both derived for swirling-dominated flow were compared. A detailed introduction of the turbulence models involved is given in the following sections.

Mathematical model
RNG k-ε model

The k-ε model is a model based on model transport equations for the turbulence kinetic energy (k) and its dissipation rate (ε). In the derivation of the k-ε model, the assumption is that the flow is fully turbulent, and the effects of molecular viscosity negligible. It is a semi-empirical model, and the derivation of the model equations relies on phenomenological considerations and empiricism. As the strengths and weaknesses of the standard k-ε model have become known, modifications have been introduced to improve its performance. The RNG k-ε model is a modified form of standard k-ε model. It is also derived from Navier-Stokes equations using a rigorous statistical technique, called "Renormalization Group Theory" (RNG) methods. Overall the RNG model resembles to the standard model, but has an additional term in its ε equation that improves the accuracy for rapidly strained flows.

The flow field inside hydrocyclones is a typical flow of rapidly strained which is of steep radial velocity and pressure gradients. Besides, the effect of swirling flow on turbulence is included in the RNG model, enhancing accuracy for the flow in hydrocyclones. The RNG theory also provides an analytical formula for turbulent Prandtl numbers, not a constant value. These features make the RNG model more accurate and reliable for resolving the swirling-dominated flow field of hydrocyclones. The RNG k-ε model is similar in form to the standard k-ε model:

$$\frac{\partial}{\partial t}(\rho k) + \frac{\partial}{\partial x_i}(\rho k u_i) = \qquad (1)$$

$$\frac{\partial}{\partial x_j}\left(\alpha_k \mu_{eff} \frac{\partial k}{\partial x_j}\right) + G_k + G_b - \rho \varepsilon - Y_M + S_k$$

and

$$\frac{\partial}{\partial t}(\rho \varepsilon) + \frac{\partial}{\partial x_i}(\rho \varepsilon u_i) = \frac{\partial}{\partial x_j}\left(\alpha_s \mu_{eff} \frac{\partial s}{\partial x_j}\right) + \qquad (2)$$

$$C_{1s}\frac{s}{k}(G_k + C_{3s}G_b) - C_{2s}\rho\frac{s^2}{k} - R_s + S_s$$

where

G_k represents the generation of turbulence kinetic energy due to the mean velocity gradients.

G_b is the generation of turbulence kinetic energy due to buoyancy.

Y_M represents the contribution of the fluctuating dilatation in compressible turbulence to the overall dissipation rate.

α_s and α_k are the inverse effective Prandtl numbers, for ε and k respectively.

S_k and S_s are the user-defined source terms.

And it is important that RNG accounts for the effects of swirl or rotation by the turbulent viscosity appropriately. If turbulence in general is affected by rotation or swirl in the mean flow, it is better to use the modification form of turbulent viscosity, μ_t:

$$\mu_t = \mu_{t0}f\left(\alpha_s, \Omega, \frac{k}{s}\right) \qquad (3)$$

where μ_{t0} is the value of turbulent viscosity calculated without the swirl modification. Ω is a characteristic swirl number, and α_s is a swirl constant that assumes different values depending on whether the flow is swirl dominated or only mildly swirling. By default, α_s is set to 0.07. But a higher value of α_s might produces better results in a strongly swriling flow fluid.

Stress-Omega Reynolds Stress Model (Omega RSM)

Different from the k-ε model, Reynolds stress model abandoning the isotropic eddy-viscosity hypothesis closes the Reynolds-averaged Navier-Stokes equations by solving transport equations for the Reynolds stresses, together with an equation for the dissipation rate. This means that seven additional transport equations are needed in 3D. As a result, it requires more CPU memory and time for each iteration. In consideration of the effects of streamline curvature, swirl, rotation, and rapid changes in strain rate in a more rigorous manner than models with one-equation and two-equation, RSM however has greater potential to give accurate predictions for complex flows theoretically.

However the RSM might not always yield results that are clearly superior to the simpler models in all classes of flows to warrant the additional computational expense, because the fidelity of RSM predictions is still limited by the closure assumptions employed to model various terms in the exact transport equations for the Reynolds stresses. But, it is preferable to use RSM when the flow features of interest are the result of anisotropy in the Reynolds stresses. The exact transport equations for the transport of the Reynolds stresses, $\rho\overline{\mu'_t\mu'_j}$ may be described as follows:

$$\frac{\partial}{\partial t}\left(\rho\overline{\mu'_t\mu'_j}\right) + C_{ij} = D_{ij}^T + D_{ij}^L + P_{ij} - \qquad (4)$$

$$P_{ij} + G_{ij} + \phi_{ij} + \varepsilon_{ij} + F_{ij}$$

This is the exact form of the Reynolds stress transport equations derived by taking moments of the exact momentum equation. It is a process wherein the exact momentum equations for the fluctuations are multiplied by the fluctuating velocities and averaged, the product then being Reynolds-averaged. However, several of the terms in the exact equation are unknown and modeling assumptions are required in order to close the equations. Of all the various terms in the Eq. (7), C_{ij}, D_{ij}^L, P_{ij} and F_{ij} do not require any modeling.

$$C_{ij} = \frac{\partial}{\partial x_k}\left(\rho u_k \overline{\mu_i \mu_j}\right) \tag{5}$$

$$D_{ij}^L = \frac{\partial}{\partial x_k}\left[\mu \frac{\partial}{\partial x_k}\left(\overline{\mu_i' \mu_j'}\right)\right] \tag{6}$$

$$P_{ij} = -\rho\left(\overline{\mu_t' \mu_k'}\frac{\partial U_j}{\partial x_k} + \overline{\mu_j' \mu_k'}\frac{\partial U_i}{\partial x_k}\right) \tag{7}$$

$$F_{ij} = -2\rho\Omega_k\left(\overline{\mu_i'\mu_m'}\varepsilon_{jkm} + \overline{\mu_t'\mu_m'}\varepsilon_{ijkm}\right) \tag{8}$$

However, D_{ij}^T, G_{ij}, ϕ_{ij} and ε_{ij} need to be modeled to close the equations.

Most importantly, for the pressure-strain term, ϕ_{ij}, modeling, there are three choices, Linear Pressure-Strain, Quadratic Pressure-Strain and Stress-Omega(the one adopted in present study). The Stress-Omega model is a stress-transport model that is based on the omega equations and LRR model. This model can provide a superior performance for modeling flows over curved surfaces and swirling flows. Also it requires no treatment of wall reflections. Except for two additional coefficients, the closure coefficients are identical to the k-ε model. The Stress-Omega model therefore is suitable for a wide range of turbulent flows. The Stress-Omega mode can be written as:

$$\phi_{ij} = -C_{1\rho}\beta_{RSM}^*\omega\left(\overline{\mu_i'\mu_j'} - \frac{2}{3}\delta_{ij}k\right) - \tag{9}$$

$$a_0\left(P_{ij} - \frac{1}{3}P_{kk}\delta_{ij}\right) - \beta_0\left(D_{ij} - \frac{1}{3}P_{kk}\delta_{ij}\right) -$$

$$k\gamma_0\left(S_{ij} - \frac{1}{3}S_{kk}\delta_{ij}\right)$$

In the case when the Reynolds Stress model is coupled with the omega equation, the dissipation tensor ε_{ij} is modeled as:

$$\varepsilon_{ij} = \frac{2}{3}\delta_{ij}\rho\beta_{RSM}^*k\omega \tag{10}$$

Meshing and computational approach

A conventional cylinder-cone hydrocyclone was modeled based on a 3-D geometry instead of 2-D plane due to its asymmetric nature at the inlet. Detailed dimensions of the hydrocyclone are illustrated in Fig. 2.
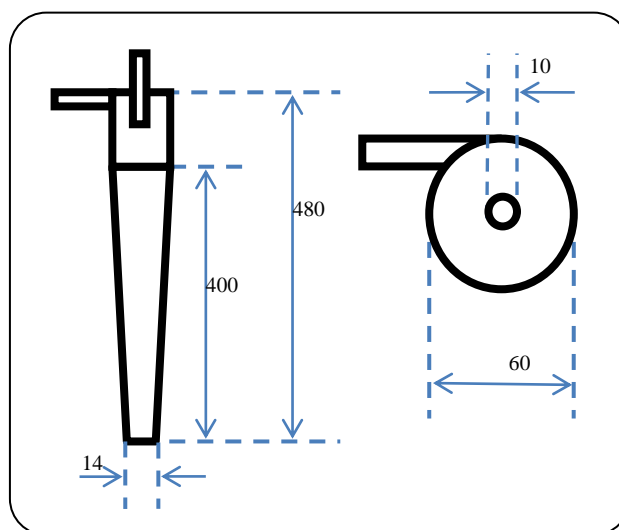

Fig. 2: Dimensions of the hydrocyclone geometry. Left: side view. Right: top view. All measures are given in millimeters.

The entire geometry was meshed by sweep method of hexahedrons, which is accessible to a faster and more accurate result in CFD. Also the hex mesh is the best to align with the flow direction which can prevent the false diffusion compared with other mesh element shapes. A fine mesh with an average skewness 0.15 was created and optimized for good predictions and reasonable calculation time. Ansys 14.0 Fluent was applied to perform the computation. The simulation was carried out in the pressure-based solver for a steady, non-gravity and one phase flow of water. For boundary conditions, velocity inlet and pressure outlet were adopted at the inlet and outlets respectively. For the turbulence model, RNG k-ε and Omega RSM were introduced separately. To solve the pressure field, SIMPLE, a pressure-velocity coupling algorithm was used. The SIMPLE algorithm uses a relationship between velocity and pressure corrections to enforce mass conservation and to obtain the pressure field. And because of the predominant centrifugal field inside the hydrocyclone body force weighted was adopted for interpolation of pressure. Second order upwind was used to the spatial discretization of other variables. During the solution, both residual criteria and point velocities (two points that were created in cylinder and cone parts separately) were monitored to ensure a desirable result. For this research, the computation would carry on until the residuals achieved 10^{-5} and the point velocity profiles monitored went straight.
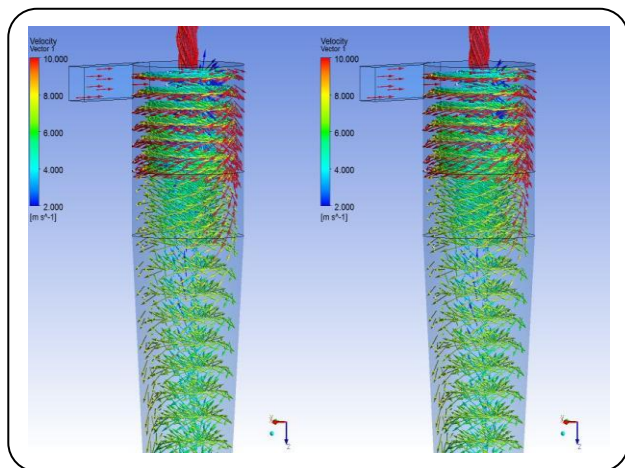
Fig. 3: Overview of velocity vectors profile (upper part only, for a magnified view). Left: RNG and right: Omega. Colored by the absolute velocity (m/s). For a clear view of velocity gradient, the scope of color legend was set to 2~10 (m/s), which means the sections with the absolute velocity more than 10m/s are all displayed as red and less than 2m/s all blue.
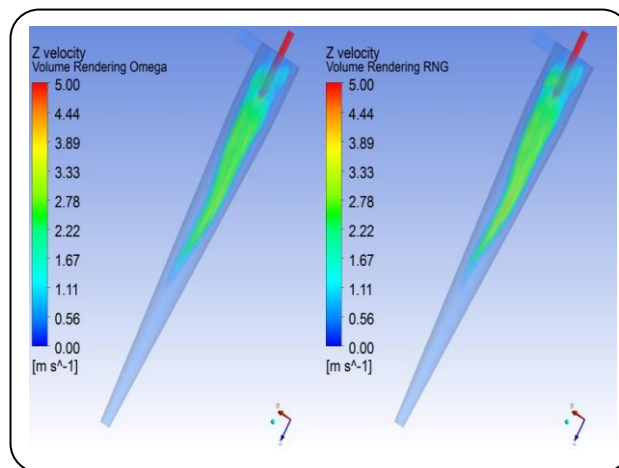

Fig. 4: Volume rendering of inner vortex. The left is obtained by Omega, the right RNG. The volume with a minus Z-velocity (moving towards the overflow tube) is colored by absolute Z-velocity. The color legend is set to 0~5 (m/s).

RESULTS AND DISCUSSION

In this section the main results yielded by RNG k-ε model and Omega RSM, which are both derived for modeling a swirling or rotational flow, were compared in details. The inlet boundary condition was defined at a velocity of 20m/s and a turbulent intensity of 10%. Overflow and underflow outlets were set as pressure-out instead of outflow, respectively designated as atmospheric plus a pressure corresponding to the local centrifugal force.

Overview of flow fields

A general feature of flow field inside the hydrocyclone is showed by velocity vectors in Fig. 3. It is easy to find that both of them present similar distributions of velocity in terms of whether the directions or the gradient. Also in both it can be observed that there are two reversed vortexes, inner and outer, formed inside the hydrocyclone.

Fig. 4 presents a direct view of the region of inner vortex (the vortex moves upward). One can see that the whole inner vortex extends from the region around the overflow tube to the middle of cone part. It is also can be observed that, in terms of both the shape and the volume of inner vortex, two models led to almost the same predictions. In other words, in describing the region of the two reversed flow inside the hydrocyclone, the RNG

and the Omega were of no obvious difference.

In all, from overview, both models yielded a similar simulation on the created liquid-liquid hydrocyclone.

Detailed view of velocity profiles

With the purpose of a further study on the detailed distinction between them, three radius lines and an axis line, showed in Fig. 5, were drawn to demonstrate different variables.

Fig. 6 gives the profiles of absolute velocity along the created lines in Fig. 5. For the axis line, generally the trend of two curves is similar, especially in the region close to outlets. But in the middle of the axis line, the velocity profile of Omega is a little smoother. Due to the existing of both inner vortex and outer vortex in the middle part of the hydrocyclone the flow pattern became complicated compared with the region near outlets. So the results yielded by two models showed a little difference. The same as axial line, one can see a similar trend of velocity profiles along each radius line. This M-type velocity profiles along radius have also been found by many former investigations [8-10].

Fig. 7 shows the contours of absolute velocity in an axial plane for different inlet velocities, 10m/s (Case A), 20m/s (Case B), 30m/s (Case C). It can be observed that, overall, similar velocity contours are given by the two models in each case. But the contour of Omega shows
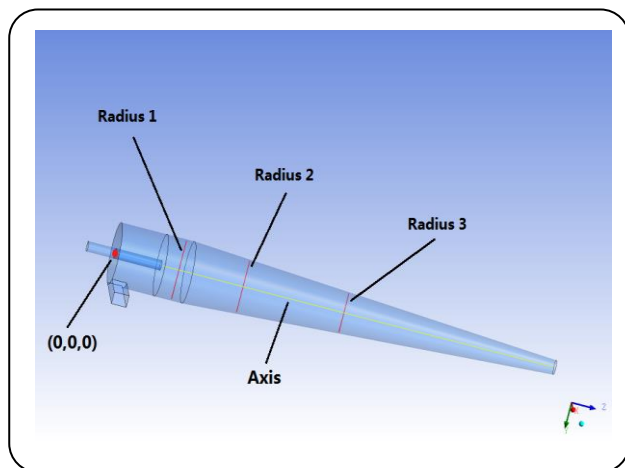
Fig. 5: Hydrocyclone with created lines. The yellow is axis line and the other three red lines are radiuses of different cross-sections. Radius 1 is in the cylinder part, while Radius 2, 3 in the cone part. A coordinates is also created, taking the center of the cap circle surface as origin (0,0,0). X direction is in accordance with the extrusion direction of inlet, Y direction is downwards the underflow outlet.

a more integral core of low-velocity. Many previous studies have proven that the core region is of both low-velocity and low-pressure, even an air core generates sometimes [11-14]. Besides, in the lower cone part, velocity field obtained by RNG shows a large gradient along radius. Due to the reduction in cross-section area of the flow passage and long residence time, in the lower cone part, the velocity gradient along the radius becomes small instead of large [15-16]. In these detailed features, Omega RSM was a little more reasonable and applicable for the prediction of the hydrocyclone.

And the increase in velocity inevitably led to a flow filed of enhancing swirling movement. However, as Fig. 7 shows, with the increasing inlet velocity the Omega RSM has performed no more obviously superior to RNG k-ε model than it has done in a relatively mild flow field. In RNG model, the turbulent viscosity, μ_t, is calculated with a swirl modification which is in order to obtain accurate Reynolds stress as the intensity of swirl changes rapidly. Therefore, with the enhancing of swirling intensity, the velocity fields produced by the two models still remained generally similar.

Mass split ratio at different inlet velocities

The mass split ratio is a key value that must be exactly appropriate for the separation requirements,

which is defined as k:

$$k = \frac{V_{overflow}}{V_{inlet}} \tag{15}$$

where $V_{overflow}$ is the volume flow of overflow, for incompressible fluid massflow as well. Likewise, V_{inlet} is the volume flow of inlet. Table 1 gives the mass split ratio of different cases. In each case, it can be observed that nearly equal massflows were solved out by two models. This is also consistent with the former finding showed in Fig. 4, which presents the similar volume of inner vortex obtained by two models, because the massflow of inlet is approximately the same as the quantity of inner vortex. In all, under different inlet velocities, there was no significant difference in the predictions of massflow banlance between RNG k-ε model and Omega RSM.

Comparison of turbulence viscosities

Fig. 8 presents the turbulent viscosity profiles along the radius lines. Different from the molecular viscosityμ, turbulent viscosity has almost no relation to the molecular diffusion, but is closely relevant to the turbulence intensity. In essence it describes the interaction of turbulent eddies. And the turbulent viscosity is proportional to turbulent kinetic energy and dissipation rate. It is easy to see that the profiles of turbulent viscosity obtained by RNG and Omega are quite different in both trend and magnitude. The red curve (computed by Omega) shows an obvious M-style. And the RNG model yielded lower results. Compared with other turbulence models, during the solution of turbulentce viscosity, in RNG model there is a smaller destruction of the dissipation rate which eventually reduces the effective viscosity. As a result, the RNG model yields a lower turbulent viscosity in rapidly strained flows [7]. And due to the weak turbulence, turbulent viscosity should be lower in the axial and near-wall region. Thus, an M-type profile of turbulent viscosity along the radius should be aligned with the reality. Additionally the RNG yielded a much lower turbulent viscosity in the region of axis than that in the near-wall region, which is not practical. For this reason, the Omega RSM was more accurate and reasonable.
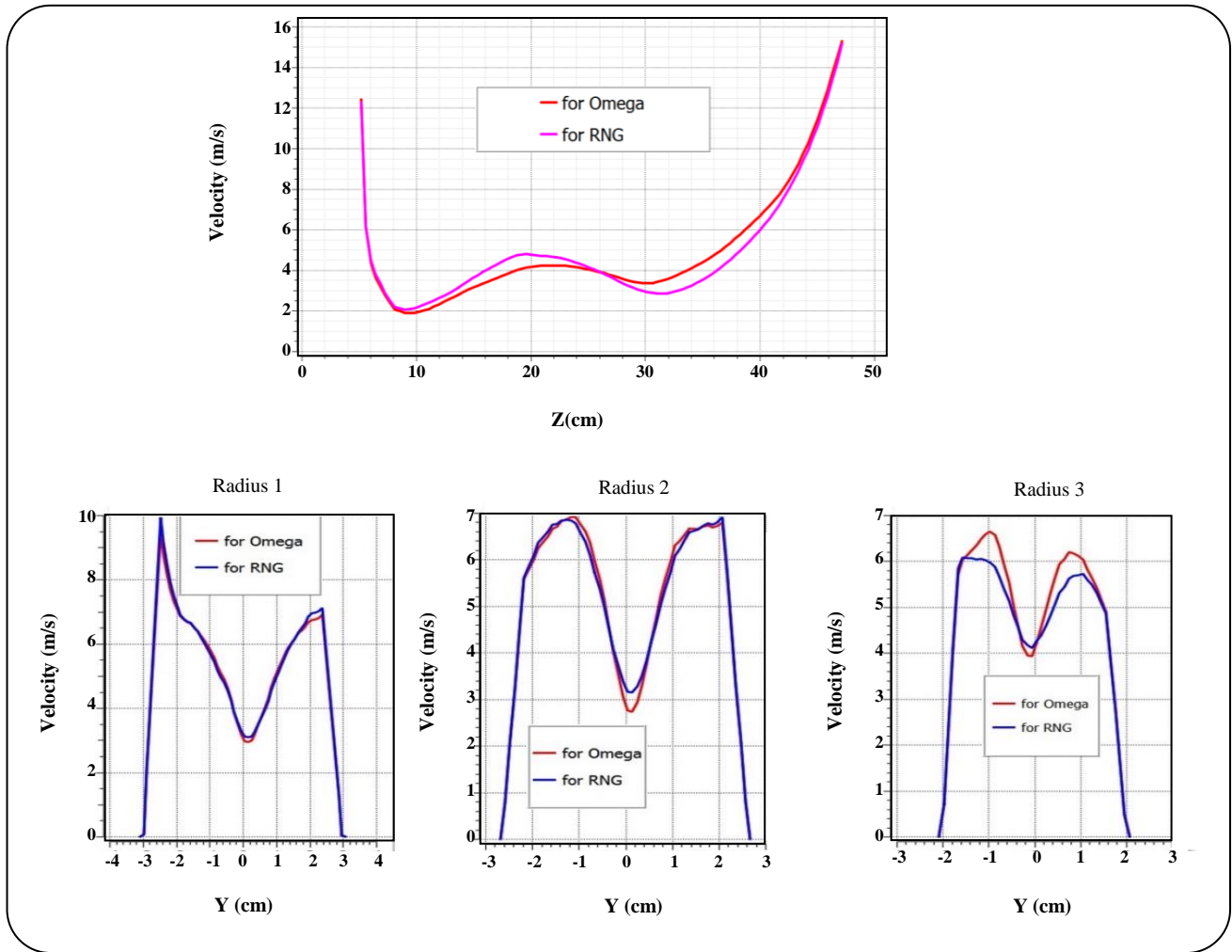
Fig. 6: The upper: Absolute velocity profile along the created axis. X-axis represents the Z-coordinates of the created axis. The lower: Absolute velocity profile along each created radius. Y-axis represents the Y-coordinates of the created radiuses.
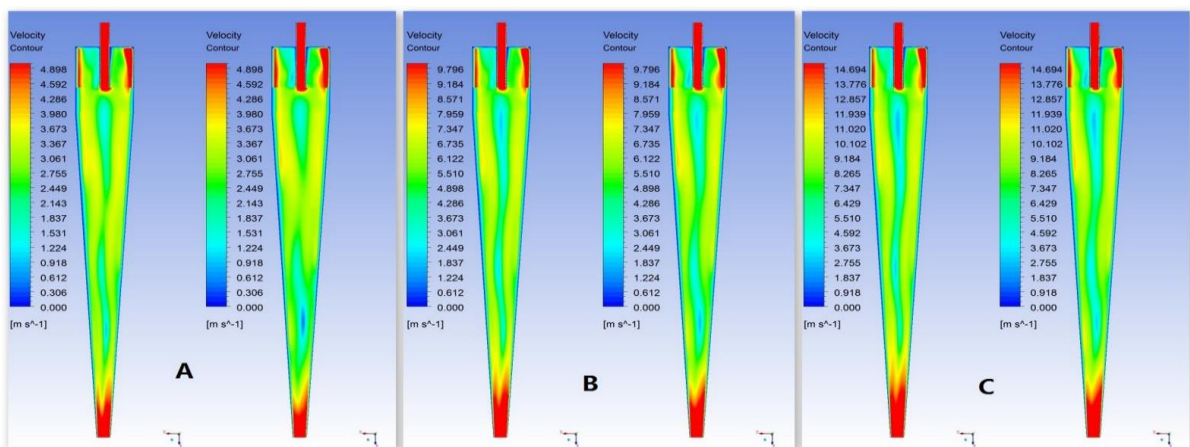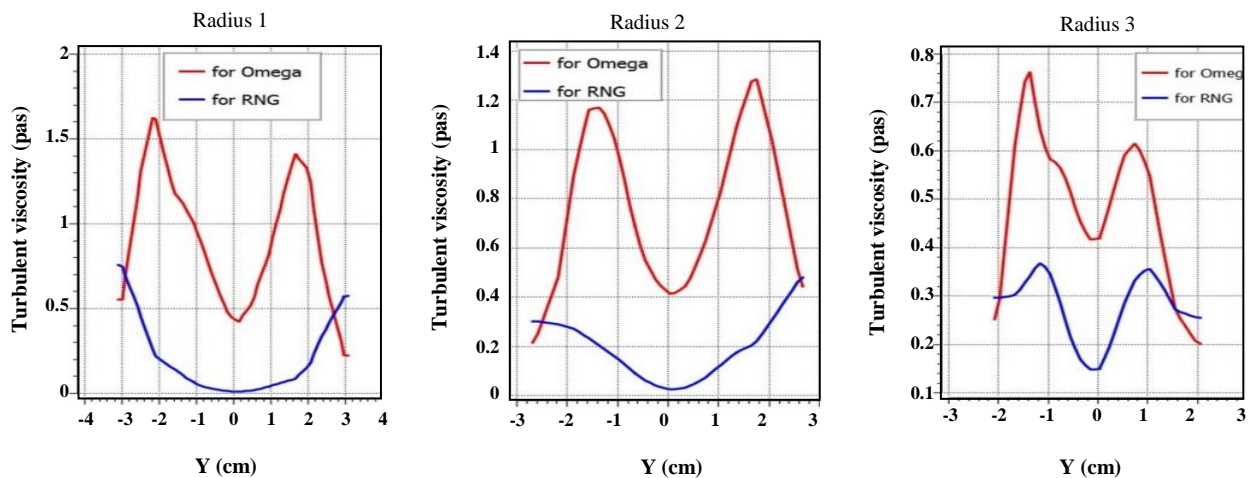

Fig. 7: Contours of absolute velocity (m/s) in axial plane, colored by absolute velocity. Case A:10m/s, case B:20m/s, case C:30m/s. In each case, the left is Omega and the right RNG.

Table 1:Mass split ratio of different inlet velocities, obtained by two models.

	Overflow (m^3/s)	Inlet (m^3/s)	Mass split ratio, %
Omega (10m/s)	0.8201	1.9165	0.4279
RNG (10m/s)	0.8201	1.9165	0.4279
Omega (20m/s)	1.3277	3.8331	0.3464
RNG (20m/s)	1.3224	3.8331	0.3450
Omega (30m/s)	1.8195	5.7496	0.3164
RNG (30m/s)	1.8057	5.7496	0.3140

Fig. 8: Turbulent viscosity profile along each created radius. Y-axis represents the length of the created radiuses.

CONCLUSIONS

In the present investigation, the Omega Reynolds Stress Model was introduced to describe the flow field inside a hydrocyclone in comparison with the RNG k-ε model. With respect to the general velocity field, mass split ratio and the volumetric fraction of two inversed vortexes, Omega RSM and RNG k-ε model gave similar predictions. And both models were qualified to capture the variation of swirling intensity. Therefore, for a qualitative analysis or design of the hydrocyclone, RNG k-ε model can be appropriate and applicable, which is accessible to faster results.

Still Omega RSM could give a more accurate prediction of turbulent viscosity as well as a better description in the core region inside the hydrocyclone for its isotropic hypothesis of turbulent viscosity, one of the major defects of the two-equation model (k-ε model), is eliminated. But behind the accuracy of the complicated Omega, it does require much more expensive computational cost. And the conclusions above are also probable to be true for many other industrial processes featuring strong turbulence and high swirling movement.

REFERENCES

[1] Chesters A.K., *J. Transactions of the Institution of Chemial Engineers*, **69**: 259-269 (1991).

[2] Bapat P.M., Tavlarides L.L., Smith G.W., *J. Chem. Eng. Sci.*, **38**: 2003-2013 (1983)

[3] Bednarski K., Listewnik J., In: "Proceedings of the Third International Conference on Hydrocyclones", Oxford, Uk, pp. 181-192 (1987).

[4] Griffiths W.D., Boysan F., *J. Aerosol Sci.*, **27**: 281-304 (1996).

[5] Narasimha M., Brennan M.S., Holtham P.N., *J. Minerals Engineering*, **20**: 414-426 (2007).

[6] Launder B.E., Spalding D.B., *J. Computer Methods in Applied Mechanics and Engineering*, **3**: 269-289 (1974).

[7] Ansys 14.0 Help

[8] Bhaskar K.U., Murthy Y.R., Raju M.R., *J. Minerals Engineering*, **20**: 60-71 (2007).

[9] Chuah T.G., Gimbun J., Choong T.S.Y., *J. Powder Technology*, **162**: 126-132 (2006).

[10] Delgadillo J.A., Rajamani R.K., *J. International journal of mineral processing*, **77**: 217-230 (2005).

[11] Cullivan J.C., Williams R.A., Cross R., *J. Chemical Engineering Research and Design*, **81**: 455-466 (2003).

[12] Cullivan J.C., Williams R.A., Dyakowski T., *J. Minerals Engineering*, **17**: 651-660 (2004).

[13] Bergström J., Vomhoff H., *J. Separation and Purification Technology*, **53**: 8-20 (2007).

[14] Doby M.J., Nowakowski A.F., Yiu I., *J. International Journal of Mineral Processing*, **86**: 18-25 (2008).

[15] Bai Z., Wang H., Tu S.T., *J. Minerals Eng.*, **22**: 319-323 (2009).

[16] Fisher M.J., Flack R.D., *J. Experiments in Fluids*, **32**: 302-312 (2002).